Synchronization of Nonlinear Circuits in Dynamic Electrical Networks With General Topologies

Sairaj V. Dhople, *Member, IEEE*, Brian B. Johnson, *Member, IEEE*, Florian Dörfler, *Member, IEEE*, and Abdullah O. Hamadeh

***Abstract*—Sufficient conditions are derived for global asymptotic synchronization in a system of identical nonlinear electrical circuits coupled through linear time-invariant (LTI) electrical networks. In particular, the conditions we derive apply to settings where: i) the nonlinear circuits are composed of a parallel combination of passive LTI circuit elements and a nonlinear voltage-dependent current source with finite gain; and ii) a collection of these circuits are coupled through either uniform or homogeneous LTI electrical networks. Uniform electrical networks have identical per-unit-length impedances. Homogeneous electrical networks are characterized by having the same effective impedance between any two terminals with the others open circuited. Synchronization in these networks is guaranteed by ensuring the stability of an equivalent coordinate-transformed differential system that emphasizes signal differences. The applicability of the synchronization conditions to this broad class of networks follows from leveraging recent results on structural and spectral properties of Kron reduction—a model-reduction procedure that isolates the interactions of the nonlinear circuits in the network. The validity of the analytical results is demonstrated with simulations in networks of coupled Chua's circuits.**

***Index Terms*—Kron reduction, nonlinear circuits, synchronization.**

I. Introduction

SYNCHRONIZATION of nonlinear electrical circuits coupled through complex networks is integral to modeling, analysis, and control in application areas such as the ac electrical grid, solid-state circuit oscillators, semiconductor laser arrays, secure communications, and microwave oscillator arrays [1], [2]. This paper focuses on global asymptotic synchronization of terminal voltages in a class of nonlinear circuits coupled through passive LTI electrical networks. We assume that the nonlinear circuits are composed of a parallel combination of a passive LTI circuit and a nonlinear voltage-dependent current source with finite gain. A collection of such identical circuits are coupled through uniform or homogeneous passive LTI electrical networks. Uniform networks have identical per-unit-length impedances and include purely resistive and lossless networks as special cases. Homogeneous electrical networks are characterized by identical effective impedances between the terminals (essentially, the impedance between any two terminals with the others open circuited). Section V provides precise definitions of these network types.

The motivation for this work stems from developing control paradigms for power electronics inverters in low-inertia microgrids based on the emergence of synchronization in complex networks of coupled heterogeneous oscillators. The key idea pertains to controlling power electronic inverters to emulate the dynamics of nonlinear limit-cycle oscillators [3], [4]. Our previous work in [4]–[6] considered the problem of controlling parallel-connected power electronics inverters to emulate the dynamics of Liénard-type oscillators. The oscillators (inverters) are coupled (connected) through the existing microgrid electrical network, and synchrony emerges in this system with no external forcing in the form of a utility grid or any communication beyond the existing physical electrical network. This paper generalizes the results in [4]–[6] by establishing synchronization conditions for a much wider class of nonlinear electrical circuits and networks.

The nonlinear-circuit models, and the uniform and homogeneous networks examined in this work offer a broad level of generality and ensure a wide applicability of the analytical results to many settings. For instance, a variety of chaotic and hyperchaotic circuits as well as nonlinear oscillators [3], [4], [7]–[12] can be modeled as a parallel connection of a linear subsystem and a nonlinear voltage-dependent current source with finite gain. Similarly, the types of networks that our results accommodate, facilitate the analysis of varied interconnections between the nonlinear circuits. In general, we study interconnecting networks that are *dynamic*, i.e., the network can contain capacitive or inductive storage elements.

We consider two broad classes of LTI electrical networks. For uniform networks, the per-unit-length line impedances can be complex (i.e., not exclusively resistive or reactive) and the network topology can be arbitrary. With regard to resistive (lossless) networks, we allow the branch resistances (respectively, reactances) and the network topology to be arbitrary. Finally, homogeneous networks are frequently encountered in engineered setups (e.g., power grid monitoring and impedance tomography), in large random networks or regular lattices, as well as in idealized settings where all terminals are electrically uniformly distributed with respect to each other [13].

The analytical approach adopted in this paper builds on previous work in [4], [14]–[16], where $\mathcal{L}_2$ methods were used to

Manuscript received October 15, 2013; revised January 24, 2014; accepted February 19, 2014. Date of current version August 26, 2014. This paper was recommended by Associate Editor Y. Uwate.

S. V. Dhople is with the Department of Electrical and Computer Engineering at the University of Minnesota, Minneapolis, MN 55455 USA (e-mail: sdhople@UMN.EDU).

B. B. Johnson is with the Power Systems Engineering Center at the National Renewable Energy Laboratory, Golden, CO 80401 USA (e-mail: brian.johnson@NREL.GOV).

F. Dörfler is with the Automatic Control Laboratory, ETH Zürich, 8092 Zürich, Switzerland (e-mail: dorfler@ETHZ.CH).

A. O. Hamadeh is with the Department of Mechanical Engineering, Massachusetts Institute of Technology, Cambridge, MA 02139 USA (e-mail: ahamadeh@MIT.EDU).

Color versions of one or more of the figures in this paper are available online at http://ieeexplore.ieee.org.

Digital Object Identifier 10.1109/TCSI.2014.2332250

analyze synchronization of dynamicaly coupled feedback systems. Our $\mathcal{L}_2$ approach offers an alternate perspective compared to a rich body of literature that has examined synchronization problems predominantly in memoryless networks through Lyapunov- and passivity-based methods [3], [17]–[25]. To investigate synchronization, the linear and nonlinear subsystems in the network of coupled nonlinear electrical circuits are compartmentalized, and a coordinate transformation is applied to recover an equivalent *differential system* that emphasizes signal differences. Once the differential $\mathcal{L}_2$ gains of the linear and nonlinear subsystems are identified, synchronization can be guaranteed by ensuring the stability of the coordinate-transformed differential system with a small-gain argument.

The suite of synchronization conditions presented in this paper generalize our previous efforts in [4] (which were limited to electrical networks with a star topology) to arbitrary network topologies. Integral to the analysis that allows us to investigate varied topologies is a model-reduction procedure called *Kron reduction* [26]. This procedure explicitly uncovers the interactions between the nonlinear electrical circuits, while systematically eliminating exogenous nodes in the network.

To summarize, the main contributions of this work are as follows. We analyze synchronization of coupled nonlinear circuits based on $\mathcal{L}_2$ methods. Our $\mathcal{L}_2$ approach readily applies to static and dynamic networks, and it offers an alternative generalized analysis path to synchronization phenomena that have been previously studied with Lyapunov- and passivity-based methods and appropriately constructed energy functions. Moreover, we leverage recent results on structural and spectral properties of Kron reduction [13] to derive synchronization conditions for complex networks of electrical circuits. A related contribution is that some key lemmas from [13] are extended from the real-valued and symmetric to the complex-symmetric (and not necessarily Hermitian) case, and we also offer converse results to some statements in [13].

The remainder of this manuscript is organized as follows. Section II establishes some mathematical preliminaries and notation. In Section III, we describe the nonlinear electrical circuits, and describe their network interactions by constructing the electrical admittance matrix that couples them. In Section IV, we formulate the problem statement and derive the differential system. Synchronization conditions for networks with and without shunt elements are then derived in Sections V and VI, respectively. Simulations-based case studies are provided in Section VII to validate the approach. We conclude the paper in Section VIII by highlighting a few pertinent directions for future work.

II. Notation and Preliminaries

Given a complex-valued N-tuple $\{u_1, \ldots, u_N\}$, denote the corresponding column vector as $u = [u_1, \ldots, u_N]^{\mathrm{T}}$, where $(\cdot)^{\mathrm{T}}$ denotes transposition (without conjugation). The Euclidean norm of a complex vector, u, is defined as $\|u\|_2 := \sqrt{u^* u}$, where $(\cdot)^*$ signifies the conjugate transpose.

Denote the $N \times N$ identity matrix as I, and the N-dimensional vectors of all ones and zeros as $\mathbf{1}$ and $\mathbf{0}$, respectively. The Moore-Penrose pseudo inverse of a matrix U is denoted by $U^{\dagger}$. Let $\mathrm{j} = \sqrt{-1}$ be the imaginary unit. We denote the Laplace transform of a continuous-time function $f(t)$ by f. Further, we denote transfer matrices by capital letters such as F. The cardinality of a finite set $\mathcal{N}$ is denoted by $|\mathcal{N}|$.

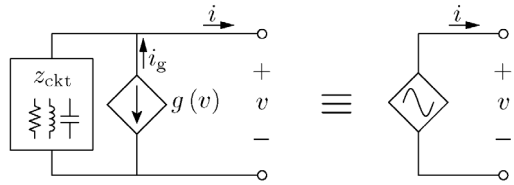

Fig. 1. Electrical schematic of the nonlinear circuit studied in this work. Each circuit is composed of a linear subsystem modeled by a passive impedance, z_{ckt}, and a nonlinear voltage-dependent current source, $g(\cdot)$. The associated circuit symbol is shown on the right.

The space of all piecewise continuous functions such that

$$\|u\|_{\mathcal{L}_2} := \sqrt{\int_0^\infty u(t)^{\mathrm{T}} u(t) \mathrm{d}t} < \infty \tag{1}$$

is denoted as $\mathcal{L}_2$. We refer to $\|u\|_{\mathcal{L}_2}$ as the $\mathcal{L}_2$ *norm* of u [27].

A causal system, $\mathcal{G}$, with input u and output y is *finite-gain $\mathcal{L}_2$ stable* if there exist finite and non-negative constants γ and η such that

$$\|y\|_{\mathcal{L}_2} =: \|\mathcal{G}(u)\|_{\mathcal{L}_2} \leq \gamma \|u\|_{\mathcal{L}_2} + \eta, \quad \forall u \in \mathcal{L}_2. \tag{2}$$

For linear systems represented by the transfer matrix $G : \mathbb{C} \to \mathbb{C}^{N \times N}$, it can be shown that the $\mathcal{L}_2$ gain of $\mathcal{G}$ is equal to the $\mathcal{H}_\infty$ norm, denoted by $\|\mathcal{G}\|_\infty$, and defined as

$$\gamma(\mathcal{G}) = \|\mathcal{G}\|_\infty := \sup_{\omega \in \mathbb{R}} \frac{\|G(\mathrm{j}\omega) u(\mathrm{j}\omega)\|_2}{\|u(\mathrm{j}\omega)\|_2} \tag{3}$$

where $\|u(\mathrm{j}\omega)\|_2 = 1$, provided that all poles of G have strictly negative real parts [28]. For a single-input single-output transfer function $g : \mathbb{C} \to \mathbb{C}$, $\gamma(\mathcal{G}) = \|\mathcal{G}\|_\infty = \sup_{\omega \in \mathbb{R}} \|g(\mathrm{j}\omega)\|_2$.

A construct we will find particularly useful in assessing signal differences is the $N \times N$ *projector matrix* [15], [20], [23], which is denoted by Π, and defined as

$$\Pi := I - \frac{1}{N} \mathbf{1}\mathbf{1}^{\mathrm{T}}. \tag{4}$$

For a vector u, we define $\widetilde{u} := \Pi u$ to be the corresponding *differential vector* [14]–[16], [20], [23].

A causal system with input u and output y is said to be *differentially finite $\mathcal{L}_2$ gain stable* if there exist finite, non-negative constants, $\widetilde{\gamma}$ and $\widetilde{\eta}$, such that

$$\|\widetilde{y}\|_{\mathcal{L}_2} \leq \widetilde{\gamma} \|\widetilde{u}\|_{\mathcal{L}_2} + \widetilde{\eta}, \quad \forall\, \widetilde{u} \in \mathcal{L}_2 \tag{5}$$

where $\widetilde{y} = \Pi y$. The differential $\mathcal{L}_2$ gain of a system provides a measure of the largest amplification of input signal differences.

The *linear fractional transformation* is the transfer matrix of the negative-feedback interconnection of two linear systems modeled by transfer matrices A and B, and it is given by [29]

$$\mathcal{F}(A(s), B(s)) := (I + A(s)B(s))^{-1} A(s). \tag{6}$$

Consider a symmetric and nonnegative matrix $A \in \mathbb{R}^{N \times N}$. Further, consider an undirected and weighted graph, with the *Laplacian matrix* L defined component-wise as: $l_{mn} = -a_{nm}$ (for off-diagonal terms) and $l_{nn} = \sum_{m=1}^{N} a_{nm}$ (for diagonal terms). The Laplacian matrix has zero row and column sums, it is symmetric and positive semidefinite, and its zero eigenvalue

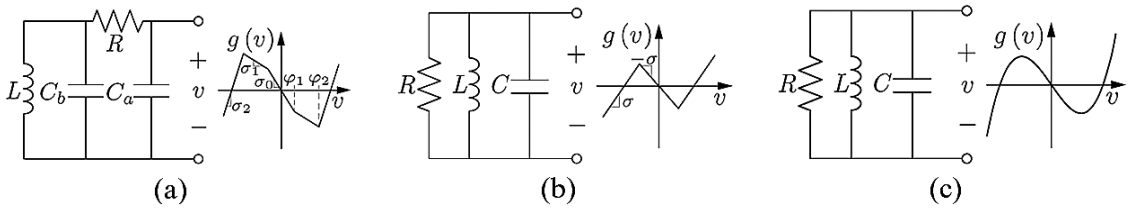

Fig. 2. The linear-subsystem impedance, $z_{\rm ckt}$, and the nonlinear voltage-dependent current source, $g(\cdot)$, illustrated for (a) Chua's circuit, (b) the Dead-zone oscillator, and (c) the Van der Pol oscillator.

is simple if and only if the graph is connected [15]. The Laplacian of a complete graph with unit weights is denoted by Γ and defined as:

$$\Gamma := NI - \mathbf{1}\mathbf{1}^{\rm T} = N\Pi. \tag{7}$$

For an electrical network with admittance matrix Y, the *effective impedance* z_{nm} between nodes n and m is the potential difference between nodes n and m, when a unit current is injected in node n and extracted from node m. In this case, the current-balance equations are $e_n - e_m = Yv$, where e_n is the canonical vector of all zeros except with a 1 in the nth position, and v is the vector of the resulting nodal voltages. The effective impedance is then

$$z_{nm} = (e_n - e_m)^{\rm T} v = (e_n - e_m)^{\rm T} Y^{\dagger}(e_n - e_m). \tag{8}$$

The effective impedance is an electric and graph-theoretic distance measure, see [13] for details and further references.

III. System of Coupled Nonlinear Electrical Circuits

We begin this section with a brief description of the type of nonlinear electrical circuits for which we derive sufficient synchronization conditions. Next, we describe the electrical network that couples the nonlinear electrical circuits.

A. Nonlinear Circuit Model

An electrical schematic of the nonlinear circuits studied in this work is depicted in Fig. 1. Each circuit has a linear subsystem composed of an arbitrary connection of passive elements described by the impedance, $z_{\rm ckt} \in \mathbb{C}$, and a nonlinear voltage-dependent current source $i_{\rm g} = -g(v)$. We require that the function $g(\cdot)$be globally Lipschitz, that is, there is a finite constant $\sigma > 0$ so that

$$g(x) - g(y) \leq \sigma(x - y) \quad \forall x, y \in \mathbb{R}. \tag{9}$$

A wide class of electrical circuits can be described within these constructs. An example is Chua's circuit [9], [30], for which the impedance $z_{\rm ckt}$ and nonlinear function $g(\cdot)$ are illustrated in Fig. 2(a). The function $g(\cdot)$ is piecewise linear, and satisfies (9). In previous work on voltage synchronization of voltage source inverters in small-scale power systems [3]–[6], we introduced a nonlinear Liénard-type dead-zone oscillator for which $z_{\rm ckt}$ and $g(\cdot)$ are illustrated in Fig. 2(b). In this case, the function $g(\cdot)$ is constructed with a negative resistance and a dead-zone function with finite slope. Some families of hyperchaotic circuits and negative-resistance oscillators can also be described by the model above, see [8], [10]–[12].

A notable example of a well-known circuit that *cannot* be described within the above framework is the Van der Pol oscillator [28]. While the linear subsystem of the Van der Pol oscillator is the same as the nonlinear dead-zone oscillator, the nonlinear voltage-dependent current is such that $g(v) \propto v^3$, and therefore does not satisfy the slope requirement in (9) (see Fig. 2(c)).

B. Electrical Network Model

The nonlinear circuits are coupled through a passive, connected, LTI electrical network. The nodes of the electrical network are collected in the set $\mathcal{A}$, and branches of the electrical network are represented by the set of edges $\mathcal{E} := \{(m,n)\} \subset \mathcal{A} \times \mathcal{A}$. Let $\mathcal{N} := \{1, \ldots, N\} \subseteq \mathcal{A}$ collect *boundary nodes* that the nonlinear circuits are connected to, and let $\mathcal{I} = \mathcal{A} \setminus \mathcal{N}$ be the set of *interior nodes* where the current injections are zero since they are not connected to the nonlinear electrical circuits. The series admittance corresponding to the $(m,n) \in \mathcal{E}$ branch is given by $y_{mn} \in \mathbb{C}$, and the shunt admittance connected between the mth node and electrical ground is given by $y_m \in \mathbb{C}$. We will assume that the boundary nodes in the set $\mathcal{N}$ are not connected to any passive shunt elements, which implies $y_m = 0$ for all $m \in \mathcal{N}$.

Denote the vectors that collect the nodal current injections and node voltages in the network by $i_{\mathcal{A}}$ and $v_{\mathcal{A}}$, respectively. The coupling between the circuits can be described by Kirchhoff's and Ohm's laws, which read in matrix-vector form as

$$i_{\mathcal{A}} = Y_{\mathcal{A}} v_{\mathcal{A}}. \tag{10}$$

In (10), $Y_{\mathcal{A}} \in \mathbb{C}^{|\mathcal{A}| \times |\mathcal{A}|}$ is the admittance matrix defined as

$$[Y_{\mathcal{A}}]_{mn} := \begin{cases} y_m + \sum_{(m,k)\in\mathcal{E}} y_{mk}, & \text{if } m = n \\ -y_{mn}, & \text{if } (m,n) \in \mathcal{E} \\ 0, & \text{otherwise,} \end{cases} \tag{11}$$

where y_m denotes the shunt admittance at node m and $y_{mn} = y_{nm}$ denotes the line admittance of branch (m,n). Notice that if the electrical network has no shunt elements, then $Y_{\mathcal{A}}$ is a singular matrix with zero row and column sums.

Let $i = [i_1, \ldots, i_N]^{\rm T}$ and $v = [v_1, \ldots, v_N]^{\rm T}$ be the vectors collecting the current injections and terminal voltages of the nonlinear circuits, and let $i_{\mathcal{I}}$ and $v_{\mathcal{I}}$ be the vectors collecting the current injections and nodal voltages for the interior nodes.[1] With this notation in place, we can rewrite (10) as

$$\begin{bmatrix} i \\ i_{\mathcal{I}} \end{bmatrix} = \begin{bmatrix} Y_{\mathcal{N}\mathcal{N}} & Y_{\mathcal{N}\mathcal{I}} \\ Y_{\mathcal{N}\mathcal{I}}^{\rm T} & Y_{\mathcal{I}\mathcal{I}} \end{bmatrix} \begin{bmatrix} v \\ v_{\mathcal{I}} \end{bmatrix}. \tag{12}$$

Since the internal nodes are only connected to passive LTI circuit elements, all the entries of $i_{\mathcal{I}}$ are equal to zero in (12).

In the following, we assume that the submatrix $Y_{\mathcal{I}\mathcal{I}}$ is nonsingular. Under this assumption, the second set of equations in (12) can be uniquely solved for the interior voltages as $v_{\mathcal{I}} = -Y_{\mathcal{I}\mathcal{I}}^{-1} Y_{\mathcal{N}\mathcal{I}}^{\rm T} v$. For RLC networks without shunt elements, the

[1]To be consistent with notation, we would have to include the subscript $\mathcal{N}$ when referring to the current and voltage vectors corresponding to the nonlinear circuits. However, we drop this subscript to ease exposition.

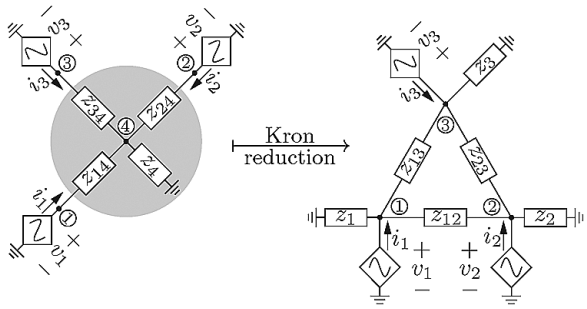

Fig. 3. Kron reduction illustrated for a representative system comprising $N = 3$ nonlinear circuits, where $\mathcal{A} = \{1, 2, 3, 4\}$, $\mathcal{N} = \{1, 2, 3\}$, and $\mathcal{I} = \{4\}$. The original electrical network described by the admittance matrix, $Y_{\mathcal{A}}$, is shaded. In this setup Kron reduction is equivalent to the well-known star-delta transformation.

matrix $Y_{\mathcal{A}}$ is irreducibly block diagonally dominant (due to connectivity of the network), and $Y_{\mathcal{I}\mathcal{I}}$ is always nonsingular [31, Corollary 6.2.27]. For RLC networks with shunt elements, it is possible to construct pathological cases where $Y_{\mathcal{I}\mathcal{I}}$ is singular, and the interior voltages $v_{\mathcal{I}}$ are not uniquely determined. In this paper, we assume that all principal submatrices are nonsingular and such pathological cases do not occur. In this case, we obtain the following equations relating the nonlinear-circuit current injections and terminal voltages:

$$i = \left(Y_{\mathcal{N}\mathcal{N}} - Y_{\mathcal{N}\mathcal{I}} Y_{\mathcal{I}\mathcal{I}}^{-1} Y_{\mathcal{N}\mathcal{I}}^{\mathrm{T}}\right) v =: Yv. \tag{13}$$

This model reduction through a *Schur complement* [32] of the admittance matrix is known as *Kron reduction* [13]. We refer to the matrix Y in (13) as the *Kron-reduced admittance matrix*. From a control-theoretic perspective, (13) is a minimal realization of the circuit (12) [33]. We remark that, even though the Kron-reduced admittance matrix Y is well-defined, it is not necessarily the admittance matrix of a passive circuit. Fig. 3 depicts an illustrative electrical network and its Kron-reduced counterpart for a system of $N = 3$ nonlinear circuits.

The results in this paper apply to Kron-reduced admittance matrices that satisfy the following two properties:

(P1) The Kron-reduced admittance matrix, Y, commutes with the projector matrix, Π, that is, $\Pi Y = Y\Pi$.

(P2) The Kron-reduced admittance matrix, Y, is normal, that is, $YY^* = Y^*Y$. Consequently, Y can be diagonalized by a unitary matrix, that is, we can write $Y = Q\Lambda Q^*$, where $QQ^* = I$ and Λ is a diagonal matrix with diagonal entries composed of the eigenvalues of Y.

We will find (P1) useful in Section IV-B to derive a system description that compartementalizes the linear and nonlinear subsystems in the network. Similarly, (P2) will be leveraged in the proof of Theorem 2 in Section V-B. We will identify classes of networks with and without shunt elements that satisfy properties (P1) and (P2) in Sections V and VI.

IV. Problem Statement and System Compartmentalization

A. Global Asymptotic Synchronization

We are interested in global asymptotic synchronization of the terminal voltages of the nonlinear circuits coupled through the

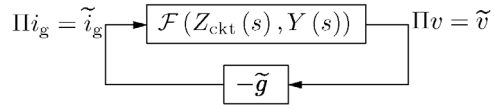

Fig. 4. Block-diagram representation of the corresponding differential system. The linear and nonlinear portions of the system are compartmentalized in $\mathcal{F}(\cdot,\cdot)$ and $\widetilde{g}$, respectively.

electrical LTI network described in Section III-B. In particular, we seek sufficient conditions that ensure

$$\lim_{t\to\infty} v_j(t) - v_k(t) = 0 \quad \forall j, k = 1, \ldots, N. \tag{14}$$

For ease of analysis, we find it useful to implement a coordinate transformation by employing the projector matrix, Π, to obtain the corresponding *differential system* emphasizing signal differences. To highlight the analytical advantages afforded by this coordinate transformation, note that:

$$\widetilde{v}(t)^{\mathrm{T}}\widetilde{v}(t) = (\Pi v(t))^{\mathrm{T}}(\Pi v(t)) = \frac{1}{2N}\sum_{j,k=1}^{N}\left(v_j(t) - v_k(t)\right)^2. \tag{15}$$

Hence, condition (14) equivalently reads as $\lim_{t\to\infty}\widetilde{v}(t) = \lim_{t\to\infty}\Pi v(t) = 0$. The coordinate transformation with the projector matrix allows us to cast the synchronization problem as a stability problem in the differential system.

Certainly, different metrics and differential coordinates other than Πv can be employed in a synchronization analysis. Our main motivation for using the projector matrix is that it naturally commutes with a particular class of admittance matrices, see property (P1).

B. Compartmentalization of Linear and Nonlinear Subsystems

In order to establish synchronization conditions, we seek a system description where the linear and nonlinear subsystems (z_{ckt} and $g(\cdot)$, respectively) in the network of coupled nonlinear circuits are clearly compartmentalized. In light of the importance of differential signals in facilitating the derivation of synchronization conditions, the compartmentalization is carried out in the corresponding differential system.

Towards this end, recall that the vectors i and v collect the current injections and terminal voltages of the nonlinear circuits. Let $i_{\mathrm{g}} := [i_{\mathrm{g}1}, \ldots, i_{\mathrm{g}N}]^{\mathrm{T}}$ be the vector that collects the currents sourced by the nonlinear voltage-dependent current sources. From Fig. 1, we see that the terminal voltage of the jth nonlinear circuit, v_j, can be expressed as

$$v_j = z_{\mathrm{ckt}}(i_{\mathrm{g}j} - i_j), \quad \forall j = 1, \ldots, N. \tag{16}$$

By collecting all v_j's, we can write

$$v = Z_{\mathrm{ckt}}(i_{\mathrm{g}} - i) = Z_{\mathrm{ckt}} i_{\mathrm{g}} - Z_{\mathrm{ckt}} Y v \tag{17}$$

where $Z_{\mathrm{ckt}} := z_{\mathrm{ckt}} I \in \mathbb{C}^{N\times N}$, and we substituted $i = Yv$ from (13). A multiplication of both sides of (17) by the projector matrix Π yields the differential terminal-voltage vector

$$\widetilde{v} = \Pi v = \Pi\left(Z_{\mathrm{ckt}}(i_{\mathrm{g}} - Yv)\right) = Z_{\mathrm{ckt}}\left(\widetilde{i}_{\mathrm{g}} - Y\widetilde{v}\right) \tag{18}$$

where we utilized $\Pi Z_{\mathrm{ckt}} = \Pi z_{\mathrm{ckt}} I = z_{\mathrm{ckt}} I\Pi = Z_{\mathrm{ckt}}\Pi$, and leveraged the commutativity property (P1).

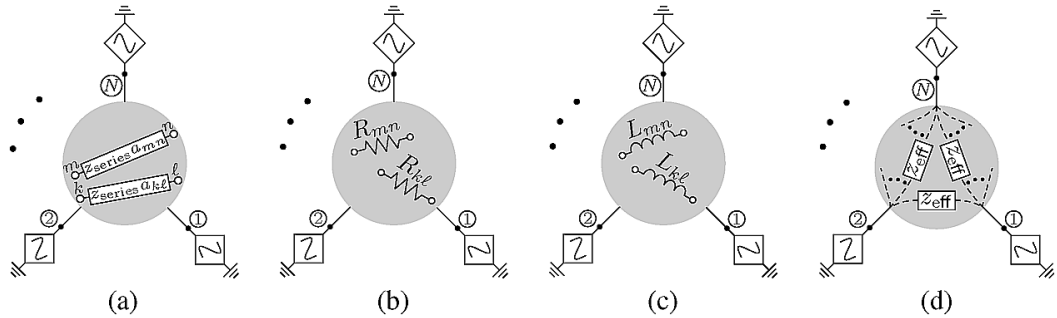

Fig. 5. Illustrating electrical networks with no passive shunt elements that are: (a) uniform, (b) resistive, (c) lossless (inductive in this particular example), and (d) homogeneous. Uniform networks have identical per-unit-length impedances, $z_{\rm series}$, such that the value of the (n,m) line impedance is expressed as the product of $z_{\rm series}$ and a_{nm}, the line length, which corresponds to the nonnegative weight from the underlying weighted Laplacian, L. As special cases, we recover resistive and lossless networks with arbitrary resistive (respectively lossless) line impedances. Finally, in homogeneous networks, the effective impedance between any two nodes is the same.

We can now isolate $\widetilde{v}$ in (18) as follows:

$$\widetilde{v} = (I + Z_{\rm ckt}Y)^{-1}Z_{\rm ckt}\widetilde{i}_{\rm g} = \mathcal{F}(Z_{\rm ckt}, Y)\widetilde{i}_{\rm g} \qquad (19)$$

where $\mathcal{F}(Z_{\rm ckt}, Y)$ is the *linear fractional transformation* that captures the negative feedback interconnection of $Z_{\rm ckt}$ and Y (see (6) for a formal definition). Using (19), we see that the corresponding differential system admits the compact block-diagram representation in Fig. 4. The linear and nonlinear portions of the system are clearly compartmentalized by $\mathcal{F}(Z_{\rm ckt}, Y)$ and the map $\widetilde{g} : \widetilde{v} \to -\widetilde{i}_{\rm g}$, respectively.

V. Global Asymptotic Synchronization In Networks Without Shunt Elements

This section focuses exclusively on synchronization in electrical networks that have no shunt elements. We begin this section by describing the class of electrical networks without shunt elements that satisfy (P1)-(P2), and then present sufficient conditions for global asymptotic synchronization of the nonlinear-circuit terminal voltages in such networks.

First, we present a result which helps us to establish that Kron-reduced admittance matrices satisfy (P1) if the originating electrical networks have no shunt elements. The following result also offers a converse statement to [13, Lemma 3.1].

Theorem 1: The following statements are equivalent:

(i) The original electrical network has no shunt elements.

(ii) The Kron-reduced network has no shunt elements.

Proof: Let us first prove the sufficiency $(i) \implies (ii)$. In the absence of shunt elements, the admittance matrix $Y_{\mathcal{A}}$ has zero row sums by construction (see (11)), that is,

$$\begin{bmatrix} \mathbf{0} \\ \mathbf{0} \end{bmatrix} = \begin{bmatrix} Y_{\mathcal{N}\mathcal{N}} & Y_{\mathcal{N}\mathcal{I}} \\ Y_{\mathcal{N}\mathcal{I}}^{\rm T} & Y_{\mathcal{I}\mathcal{I}} \end{bmatrix} \begin{bmatrix} \mathbf{1} \\ \mathbf{1} \end{bmatrix}. \qquad (20)$$

An elimination of the second set of equations in (20) results in $(Y_{\mathcal{N}\mathcal{N}} - Y_{\mathcal{N}\mathcal{I}}Y_{\mathcal{I}\mathcal{I}}^{-1}Y_{\mathcal{N}\mathcal{I}}^{\rm T})\mathbf{1} = Y\mathbf{1} = \mathbf{0}$, that is, Y has zero row sums (and zero column sums due to closure of symmetry under the Schur complement [32]). By construction of the admittance matrix in (11), it follows that the Kron-reduced electrical network corresponding to Y has no shunt elements.

We now prove the converse statement $(ii) \implies (i)$ by proving its negation $\neg(i) \implies \neg(ii)$, that is, an original network with shunt elements always leads to a Kron-reduced network with shunt elements. Consider the augmented matrix $\widehat{Y}_{\mathcal{A}}$ associated with $Y_{\mathcal{A}}$, which is obtained by modeling the ground as an additional node i with index $|\mathcal{A}| + 1$ and fixed (zero) voltage (see Appendix A for more details on the augmentation). Then $\widehat{Y}_{\mathcal{A}}$ is the admittance matrix associated to a network without shunt elements and $\widehat{Y}_{\mathcal{A}}\mathbf{1} = \mathbf{0}$. By the reasoning (i) $\implies$ (ii) above, the associated Kron-reduced matrix $\widehat{Y}$ has no shunt elements and $\widehat{Y}\mathbf{1} = \mathbf{0}$. Since Kron-reduction and augmentation commute (see Lemma 5 in Appendix A), the reduced network with admittance matrix Y obtained by removing the grounded node (that is removing the column and row with index $N+1$ from $\widehat{Y}$) does not have zero row sums. Equivalently, the Kron-reduced network has shunt elements. ■

Corollary 1: If the original electrical network has no shunt elements, then property (P1) holds, that is, Y commutes with Π.

Proof: If the original network has no shunt elements, then the Kron-reduced network has no shunt elements. Thus, Y has zero row and column sums, and Y commutes with Π. ■

A. Identifying Electrical Networks that Satisfy (P1)-(P2)

The synchronization criteria we develop within this section apply to the following classes of networks:

(i) *networks with uniform line characteristics* [34], in which the branch admittances are given $y_{nm} = y_{\rm series}a_{nm}$ for all $(n,m) \in \mathcal{E}$, where $a_{nm} \in \mathbb{R}$ is real-valued and $y_{\rm series} \in \mathbb{C} \setminus \{0\}$ is identical for every branch (see Figs. 5(a)–(c));

(ii) *homogeneous networks* [13], in which the effective impedances are identical for all boundary nodes:, $z_{nm} =: z_{\rm eff} = r + {\rm j}x$, $r, x \in \mathbb{R}$, $\forall n, m \in \mathcal{N}$ (see Fig. 5(d)).

For these networks, we next derive the Kron-reduced admittance matrices and demonstrate compliance to (P2).

We first focus on networks with uniform line characteristics, which physically correspond to networks for which all branches are made of the same material [34], i.e., the admittance of each branch (n,m) depends on its constant per-unit-length admittance, $y_{\rm series} \in \mathbb{C}$, and its length, $a_{nm} > 0$ (see Fig. 5(a)). Notice that these networks include as special cases resistive networks (Fig. 5(b)) and lossless networks (Fig. 5(c)) for which $y_{\rm series}$ is real-valued or purely imaginary, respectively. For these networks, we can express $Y_{\mathcal{A}} = y_{\rm series} \cdot L_{\mathcal{A}}$, where $L_{\mathcal{A}}$ is a symmetric, positive semidefinite, and real-valued Laplacian matrix. We have the following result:

Lemma 1: Consider a network with uniform line characteristics, that is, $Y_{\mathcal{A}} = y_{\rm series} \cdot L_{\mathcal{A}}$, where $L_{\mathcal{A}} \in \mathbb{R}^{|\mathcal{A}|\times|\mathcal{A}|}$ is a real-valued Laplacian matrix and $y_{\rm series} \in \mathbb{C}$. Then, the Kron-

reduced network has uniform line characteristics with the Kron-reduced admittance matrix given by

$$Y = y_{\text{series}} L \tag{21}$$

where $L = L_{\mathcal{N}\mathcal{N}} - L_{\mathcal{N}\mathcal{I}} L_{\mathcal{I}\mathcal{I}}^{-1} L_{\mathcal{N}\mathcal{I}}^{\mathrm{T}}$.

The proof of Lemma 1 follows by direct construction of the Kron-reduced matrix and due to the closure properties of Kron reduction [13, Lemma 3.1]. Due to the special form of the Kron-reduced admittance matrix in (21), it follows that Y is diagonalizable with a unitary matrix. We conclude that (P2) is satisfied by Kron-reduced matrices for which the original electrical network has uniform line characteristics.

To address homogeneous networks, we recall from [13, Theorem III.4] that (in the purely resistive case) a sparse electrical network becomes denser under Kron reduction and even complete under mild connectivity assumptions. However, the branch admittances in the reduced network are still heterogeneous and reflect the topology and electrical properties of the original network. In the following result, we show that for a homogeneous original network, the associated Kron-reduced network is characterized by identical branch admittances.

Lemma 2: The following statements are equivalent:

(i) The original network is homogeneous: for all boundary nodes $n, m \in \{1, \ldots, N\}$, the pairwise effective impedances take the uniform value $z_{nm} = z_{\text{eff}} \in \mathbb{C} \setminus \{0\}$.

(ii) The Kron-reduced network is complete and the branch admittances take the uniform value $y_{\text{series}} \in \mathbb{C} \setminus \{0\}$. Equivalently, the Kron-reduced admittance matrix is

$$Y = y_{\text{series}} \Gamma \tag{22}$$

where $\Gamma = NI - \mathbf{1}\mathbf{1}^{\mathrm{T}}$ is the Laplacian matrix of the complete graph.

If statements (i) and (ii) are true, then $z_{\text{eff}} = 2/N y_{\text{series}}$.

Lemma 2 is obtained as a direct corollary to Theorem 4 in Appendix A. Since the Laplacian of the complete graph is $\Gamma = N\Pi$, it commutes with the projector matrix Π. Finally, notice that since the Kron-reduced admittance matrix Y in the homogeneous case (22) is a special case of the Kron-reduced admittance matrix for the network with uniform line characteristics (21), it follows that Kron-reduced admittance matrices for homogeneous electrical networks satisfy (P2).

B. Sufficient Condition for Global Asymptotic Synchronization

This subsection derives sufficient conditions to ensure global asymptotic synchronization in the network of coupled nonlinear circuits described in Section V-A.

We remark that, in principle, any $\mathcal{L}_p$ norm can be used in the subsequent derivations, so long as the corresponding induced norm can be explicitly calculated for the linear fractional transformation. Two options that have readily calculable induced norms are the $\mathcal{L}_2$ norm (with the $\mathcal{H}_\infty$ norm serving as the induced norm) and the $\mathcal{L}_\infty$ norm (with the $\mathcal{H}_1$ norm serving as the induced norm). Our choice of the $\mathcal{L}_2$ norm is motivated by the fact that we can ensure the difference between the terminal voltages asymptotically tends to zero, hence implying synchronization. On the other hand, the $\mathcal{L}_\infty$ norm would imply that there is a finite bound on the maximal difference between the terminal voltages, which is not sufficient to ensure synchronization.

First, we present a lemma that establishes an upper bound on the differential $\mathcal{L}_2$ gain of the function $g(\cdot)$, that governs the nonlinear voltage-dependent current sources.

Lemma 3 ([4, Lemma 1]): The differential $\mathcal{L}_2$ gain of $g(\cdot)$ is finite, and upper bounded by σ:

$$\widetilde{\gamma}(g) := \frac{\|\widetilde{i}_{\mathrm{g}}\|_{\mathcal{L}_2}}{\|\widetilde{v}\|_{\mathcal{L}_2}} \leq \sigma. \tag{23}$$

We now provide a sufficient synchronization condition for the case where the nonlinear circuits are connected in networks with uniform line characteristics. Homogeneous networks follow as a special case.

Theorem 2: Suppose the electrical network that couples the system of N identical nonlinear circuits has no shunt elements, and has uniform line characteristics. Let the Kron-reduced admittance matrix be of the form $Y = y_{\text{series}} L$ as in (21). The terminal voltages of the nonlinear circuits synchronize in the sense of (14) if for all $j \in \{2, \ldots, N\}$

$$\left\| \mathcal{F}\left(z_{\text{ckt}}(\mathrm{j}\omega), y_{\text{series}}(\mathrm{j}\omega)\lambda_j\right) \right\|_\infty \sigma < 1 \tag{24}$$

where λ_j, $j \in \{2, \ldots, N\}$, are the nonzero eigenvalues of the Laplacian matrix L.

For a homogeneous network without shunt elements, the Kron-reduced matrix is $Y = y_{\text{series}}\Gamma$. Since the eigenvalues of the complete Laplacian Γ, are $\lambda_1 = 0$ and $\lambda_2 = \cdots = \lambda_N = N$, the synchronization condition (24) reduces to

$$\left\| \mathcal{F}\left(z_{\text{ckt}}(\mathrm{j}\omega), y_{\text{series}}(\mathrm{j}\omega)N\right) \right\|_\infty \sigma < 1. \tag{25}$$

For purely resistive networks the synchronization condition (24) has to be evaluated only for λ_2. The second-smallest eigenvalue λ_2 of the Laplacian matrix is known as the *algebraic connectivity*, and it is a spectral connectivity measure [35]. It can be shown that the algebraic connectivity in a resistive Kron-reduced network upper-bounds the algebraic connectivity in the original network [13, Theorem III.5]. Hence, condition (24) implies that the nonlinear circuits should be sufficiently strongly connected, which is aligned with synchronization results in complex oscillator networks with a static interconnection topology (i.e., with only resistive elements) and without unstable internal oscillator dynamics (e.g., passive oscillator subsystems) [2]. On the other hand, if the interconnecting network is *dynamic*, e.g., if it contains capacitive or inductive storage elements, then the synchronization condition (24) needs to be evaluated for all nonzero network modes λ_j, $j \in \{2, \ldots, N\}$.

Proof of Theorem 2: Consider the block-diagram of the differential system in Fig. 4. From Lemma 3, we have

$$\|\widetilde{i}_{\mathrm{g}}\|_{\mathcal{L}_2} \leq \sigma \|\widetilde{v}\|_{\mathcal{L}_2}. \tag{26}$$

For the linear fractional transformation, we can write

$$\|\widetilde{v}\|_{\mathcal{L}_2} \leq \widetilde{\gamma}\left(\mathcal{F}(Z_{\text{ckt}}, Y)\right) \|\widetilde{i}_{\mathrm{g}}\|_{\mathcal{L}_2} + \eta \tag{27}$$

for some non-negative η, where $\widetilde{\gamma}(\mathcal{F}(Z_{\text{ckt}}, Y))$ denotes the differential $\mathcal{L}_2$ gain of the linear fractional transformation. By combining (26) and (27), we arrive at

$$\|\widetilde{v}\|_{\mathcal{L}_2} \leq \widetilde{\gamma}\left(\mathcal{F}(Z_{\text{ckt}}, Y)\right) \sigma \|\widetilde{v}\|_{\mathcal{L}_2} + \eta. \tag{28}$$

By isolating $\|\widetilde{v}\|_{\mathcal{L}_2}$ from (28), we can write

$$\|\widetilde{v}\|_{\mathcal{L}_2} \leq \frac{\eta}{1-\widetilde{\gamma}\left(\mathcal{F}(Z_{\rm ckt},Y)\right)\sigma} \tag{29}$$

provided that the following condition holds

$$\widetilde{\gamma}\left(\mathcal{F}(Z_{\rm ckt},Y)\right)\sigma < 1. \tag{30}$$

If (30) holds true, then we have $\widetilde{v} \in \mathcal{L}_2$. It follows from Barbalat's lemma [14]–[16] that $\lim_{t\to\infty}\widetilde{v}(t) = \mathbf{0}$. Hence, if the network of nonlinear circuits satisfies the condition (30), global asymptotic synchronization can be guaranteed.

In the remainder of the proof, we establish an equivalent condition for (30). By definition of the differential $\mathcal{L}_2$ gain of the linear fractional transformation, we can express

$$\begin{aligned}
&\widetilde{\gamma}\left(\mathcal{F}(Z_{\rm ckt},Y)\right)\\
&=\widetilde{\gamma}\left(\mathcal{F}(z_{\rm ckt}I,Y)\right)\\
&=\sup_{\omega\in\mathbb{R}}\frac{\left\|\mathcal{F}\left(z_{\rm ckt}(\mathrm{j}\omega)I,Y(\mathrm{j}\omega)\right)\widetilde{i}_{\rm g}(\mathrm{j}\omega)\right\|_2}{\left\|\widetilde{i}_{\rm g}(\mathrm{j}\omega)\right\|_2}\\
&=\sup_{\omega\in\mathbb{R}}\frac{\left\|\left(I+z_{\rm ckt}(\mathrm{j}\omega)Y(\mathrm{j}\omega)\right)^{-1}z_{\rm ckt}(\mathrm{j}\omega)\widetilde{i}_{\rm g}(\mathrm{j}\omega)\right\|_2}{\left\|\widetilde{i}_{\rm g}(\mathrm{j}\omega)\right\|_2}\\
&=\sup_{\omega\in\mathbb{R}}\frac{\left\|Q(I+z_{\rm ckt}(\mathrm{j}\omega)y_{\rm series}(\mathrm{j}\omega)\Lambda)^{-1}z_{\rm ckt}(\mathrm{j}\omega)Q^{\rm T}\widetilde{i}_{\rm g}(\mathrm{j}\omega)\right\|_2}{\left\|Q^{\rm T}\widetilde{i}_{\rm g}(\mathrm{j}\omega)\right\|_2}
\end{aligned} \tag{31}$$

where we made use of property (P2) to diagonalize the admittance matrix as $Y = y_{\rm series}L = y_{\rm series}Q\Lambda Q^{\rm T}$, where Q is unitary and Λ is a diagonal matrix containing the real-valued and nonnegative eigenvalues of the Laplacian matrix L.

Since the Kron-reduced network has no shunt elements connected to ground, the row and column sums of Y are zero. Furthermore, since the Kron-reduced network is connected, Y has a single zero eigenvalue. Analogous comments apply to L and we obtain $\lambda_1 = 0$ with corresponding eigenvector $q_1 = (1/\sqrt{N})\mathbf{1}$. Finally, since $\mathbf{1}^{\rm T}\Pi = \mathbf{0}^{\rm T}$, we can express

$$Q^{\rm T}\widetilde{i}_{\rm g} = Q^{\rm T}\Pi i_{\rm g} = [0,p]^{\rm T} \tag{32}$$

where $p \in \mathbb{C}^{N-1}$ is made of the non-zero elements of $Q^{\rm T}\Pi i_{\rm g}$.

Using the observation in (32) and denoting the diagonal matrix with entries composed of the non-zero eigenvalues of Y by Λ_{N-1}, we can simplify (31) as follows:

$$\begin{aligned}
&\widetilde{\gamma}\left(\mathcal{F}(z_{\rm ckt}I,Y)\right)\\
&=\sup_{\omega\in\mathbb{R}}\frac{\left\|\left(I_{N-1}+z_{\rm ckt}(\mathrm{j}\omega)y_{\rm series}(\mathrm{j}\omega)\Lambda_{N-1}\right)^{-1}z_{\rm ckt}(\mathrm{j}\omega)p(\mathrm{j}\omega)\right\|_2}{\|p(\mathrm{j}\omega)\|_2}\\
&=\max_{j=2,\ldots,N}\sup_{\omega\in\mathbb{R}}\left|\frac{z_{\rm ckt}(\mathrm{j}\omega)}{1+z_{\rm ckt}(\mathrm{j}\omega)y_{\rm series}(\mathrm{j}\omega)\lambda_j}\right|.
\end{aligned} \tag{33}$$

By combining (33) and (30), we arrive at condition (24). ■

VI. Global Asymptotic Synchronization in Networks With Shunt Elements

In this section, we explore the family of electrical networks with shunt elements for which sufficient synchronization conditions similar to (24) can be derived.

A. Identifying Electrical Networks That Satisfy (P1)-(P2)

Consider the case of a Kron-reduced network, where—in addition to a single nonlinear circuit—each node $m \in \mathcal{N}$ in the network is connected to an identical shunt admittance $y_m = y_{\rm shunt}$. In this case, the Kron-reduced admittance matrix is

$$Y = y_{\rm shunt}I + Y' \tag{34}$$

where Y' corresponds to the admittance matrix that captures the coupling between the nonlinear circuits. By construction Y' does not include shunt elements and its row and column sums are zero. If the network modeled by such a Y' has uniform line characteristics (as in Section V-A), we obtain

$$Y = y_{\rm shunt}I + y_{\rm series}L \tag{35}$$

where L is the associated real-valued, symmetric Laplacian matrix. Clearly, Y as in (35) satisfies properties (P1) and (P2).

In general, it is difficult to identify networks that admit Kron-reduced admittance matrices of the form in (34) or even (35). However, we can identify a family of electrical networks that admit Kron-reduced admittance matrices of the same form as (35). Towards this end, we first present a result on Kron reduction of homogeneous networks with shunt elements.

Lemma 4: The following statements are equivalent:

(i) The original network is homogeneous: for all boundary nodes $n, m \in \{1,\ldots,N\}$, the pairwise effective impedances take the uniform value $z_{nm} = z_{\rm eff-series} \in \mathbb{C}\setminus\{0\}$ and the effective impedances to electrical ground (denoted by the node, $N+1$) take the uniform value $z_{n(N+1)} = z_{\rm eff-shunt} \in \mathbb{C}\setminus\{0\}$, with $z_{\rm eff-series}/z_{\rm eff-shunt} \neq 2N/(N-1)$.

(ii) The branch and shunt admittances in the Kron-reduced network are uniform, that is, there are $y_{\rm series} \in \mathbb{C}\setminus\{0\}$ and $y_{\rm shunt} \in \mathbb{C}\setminus\{0\}$, with $y_{\rm shunt} \neq -Ny_{\rm series}$, such that

$$Y = y_{\rm shunt}I + y_{\rm series}\Gamma. \tag{36}$$

If statements (i) and (ii) are true, then

$$\begin{aligned}
y_{\rm series} &= \frac{2}{2Nz_{\rm eff-shunt} - (N-1)z_{\rm eff-series}}\\
y_{\rm shunt} &= \frac{2(z_{\rm eff-series} - 2z_{\rm eff-shunt})}{z_{\rm eff-series}\left((N-1)z_{\rm eff-series} - 2Nz_{\rm eff-shunt}\right)}.
\end{aligned} \tag{37}$$

Lemma 4 is obtained as a direct corollary to Theorem 4 in Appendix A, by inverting the constitutive relations between admittances and effective impedances. The parametric assumption $y_{\rm shunt} \neq -Ny_{\rm series}$ (respectively, $z_{\rm eff-series}/z_{\rm eff-shunt} \neq 2N/(N-1)$) is practically not restrictive: it is violated only in pathological cases, e.g., when a capacitive (respectively inductive) shunt load compensates exactly for N inductive (respectively capacitive) line flows.

The admittance matrix Y in (36) satisfies (P1) and (P2), and it is clearly a special case of (34), with $Y' = y_{\rm series}\Gamma$. While the formulation in (36) is more restrictive, Lemma 4 identifies the *unique* class of electrical networks that admit Kron-reduced matrices of the form (36). An illustration of a Kron-reduced electrical network recovered from a homogeneous originating electrical network is depicted in Fig. 6.

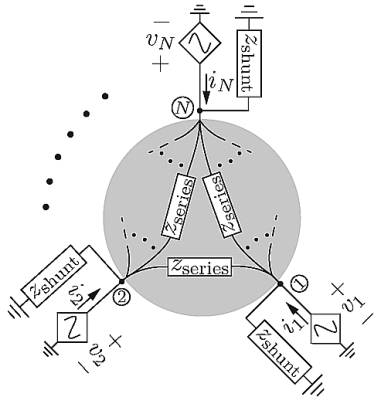

Fig. 6. Kron-reduced electrical network recovered from a homogeneous originating network. The shaded region captures the inter-circuit interactions through identical line impedances that are equal to $z_{\rm series}$. All the shunt impedances are equal to $z_{\rm shunt}$.

B. Sufficient Condition for Global Asymptotic Synchronization

We now present sufficient conditions for global asymptotic synchronization for the cases where the Kron-reduced admittance matrices are given by (35), or as a special case, by (36).

Corollary 2: Suppose the electrical network that couples the system of N identical nonlinear circuits admits a Kron-reduced admittance matrix given by (35), where the network corresponding to L has uniform line characteristics and no shunt elements connected to ground. The terminal voltages of the nonlinear circuits synchronize in the sense of (14) if for all $j \in \{2, \ldots, N\}$

$$\left\| \mathcal{F}\left(z_{\rm eq}(\mathrm{j}\omega), y_{\rm series}(\mathrm{j}\omega)\lambda_j\right) \right\|_\infty \sigma < 1 \tag{38}$$

where λ_j, $j \in \{2, \ldots, N\}$, are the nonzero eigenvalues of the Laplacian matrix L, and $z_{\rm eq}$ is the equivalent impedance of the parallel combination of $z_{\rm shunt} := y_{\rm shunt}^{-1}$ and $z_{\rm ckt}$ given by

$$z_{\rm eq} := \frac{z_{\rm shunt} z_{\rm ckt}}{z_{\rm shunt} + z_{\rm ckt}}. \tag{39}$$

Proof: The proof for this corollary follows along the same lines as that for Theorem 2. In particular, if (30) holds, then synchronization is guaranteed. Now, consider that with $Y = y_{\rm shunt} I + y_{\rm series} L$, we have that

$$\begin{aligned} \mathcal{F}(Z_{\rm ckt}, Y) &= (I + Z_{\rm ckt} Y)^{-1} Z_{\rm ckt} \\ &= \left(I + Z_{\rm ckt}(y_{\rm shunt} I + y_{\rm series} L)\right)^{-1} Z_{\rm ckt} \\ &= \left(I + \frac{z_{\rm shunt} z_{\rm ckt}}{z_{\rm shunt} + z_{\rm ckt}} y_{\rm series} L\right)^{-1} \frac{z_{\rm shunt} z_{\rm ckt}}{z_{\rm shunt} + z_{\rm ckt}} I \\ &= \mathcal{F}(z_{\rm eq} I, y_{\rm series} L), \end{aligned} \tag{40}$$

where the last line in (40) follows from the definition of the linear fractional transformation (6), and the definition of $z_{\rm eq}$ in (39). By repeating the reasoning as in the proof of Theorem 2, we obtain

$$\begin{aligned} \widetilde{\gamma}\left(\mathcal{F}(Z_{\rm ckt}, Y)\right) &= \widetilde{\gamma}\left(\mathcal{F}(z_{\rm eq} I, y_{\rm series} L)\right) \\ &= \max_{j=2,\ldots,N} \sup_{\omega \in \mathbb{R}} \left| \frac{z_{\rm eq}(\mathrm{j}\omega)}{1 + z_{\rm eq}(\mathrm{j}\omega) y_{\rm series}(\mathrm{j}\omega)\lambda_j} \right|. \end{aligned} \tag{41}$$

The claimed synchronization condition (38) then follows by combining (30) and (41). ∎

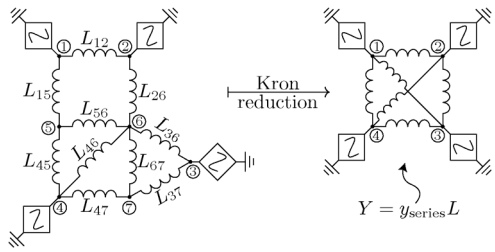

Fig. 7. Schematic of lossless inductive network and the Kron-reduced counterpart examined in Section VII-A. This is an example of a network with uniform line characteristics (see Section V), in that the Kron-reduced admittance matrix can be expressed as $Y = y_{\rm series} L$, where L is a weighted, real-valued, symmetric Laplacian matrix.

If the original electrical network coupling the N identical nonlinear circuits admits a Kron-reduced admittance matrix of the form (36), the synchronization condition (38) simplifies to

$$\left\| \mathcal{F}\left(z_{\rm eq}(\mathrm{j}\omega), y_{\rm series}(\mathrm{j}\omega) N\right) \right\|_\infty \sigma < 1. \tag{42}$$

This follows from the fact that the eigenvalues of the complete Laplacian Γ are given by $\lambda_1 = 0$ and $\lambda_2 = \ldots = \lambda_N = N$.

VII. Case Studies

We now present three simulation case studies to validate the synchronization conditions in some illustrative LTI electrical networks. In the first two case studies, we consider networks of *Chua's circuits* [30]. The nonlinear voltage-dependent current source in Chua's circuit is illustrated in Fig. 2(a), and the impedance of the linear subsystem is given by

$$z_{\rm ckt}(s) = \frac{RLC_{\rm a}C_{\rm b}s^3 + LC_{\rm a}s^2 + RC_{\rm a}s}{RLC_{\rm a}C_{\rm b}s^3 + \left(C_{\rm a}^2 + LC_{\rm b} + LC_{\rm a}\right)s^2 + RC_{\rm a}s + 1}. \tag{43}$$

The parameters of the constituent linear-circuit elements in Chua's circuit utilized in both case studies are adopted from [30], and listed in Appendix B. With the choice of circuit parameters, it follows that $\sigma = \sigma_2$.

In the third case study, we examine the impact of the underlying network topology and the number of nodes in the network on the feasibility of guaranteeing the asymptotic synchronization of periodic waveforms for a collection of *dead-zone oscillators* [4]. The nonlinear voltage-dependent current source in the dead-zone oscillator circuit is illustrated in Fig. 2(b), and the linear subsystem is given by

$$z_{\rm ckt}(s) = \frac{RLs}{RLCs^2 + Ls + R}. \tag{44}$$

The parameters of the constituent linear-circuit elements in the dead-zone oscillator circuit are listed in Appendix D.

A. Lossless Inductive Network Without Shunt Elements

The network topology examined here is illustrated in Fig. 7. This is an example of a network with uniform line characteristics (see Section V-A). Following Lemma 1, we obtain the Kron-reduced network (also illustrated in Fig. 7) with admittance matrix given by $Y = y_{\rm series} L$, where L is a weighted, real-valued, symmetric Laplacian matrix. The sufficient synchronization condition for this case is given by (24).

For the first set of network parameters in Appendix C, we get $\left\| \mathcal{F}(z_{\rm ckt}(\mathrm{j}\omega), y_{\rm series}^{-1}(\mathrm{j}\omega)\lambda_j \right\|_\infty \sigma < 1$, $j = 2, 3, 4$, which implies that the terminal voltages of the Chua's circuits are guaranteed to synchronize. We confirm this with time-domain simulations.

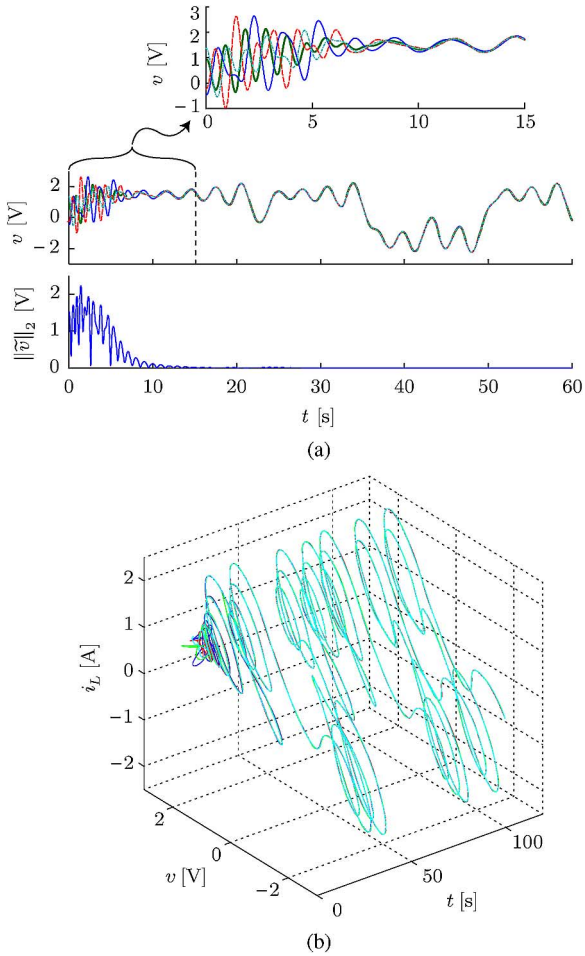

Fig. 8. Synchronization of terminal voltages in Chua's circuits. (a) Terminal voltages $v(t)$ and synchronization error $\|\widetilde{v}(t)\|_2$. (b) Chaotic double-scroll attractor in the asymptotic limit.

Fig. 8(a) illustrates the terminal voltages and the voltage synchronization error, with the inset capturing a close-up during startup with nonidentical initial conditions as the voltages begin to pull into phase. Fig. 8(b) depicts a three-dimensional view of the internal states of the Chua's circuits as a function of time, and clearly demonstrates the chaotic double-scroll attractor [30] in the asymptotic limit.

Now consider the second set of network parameters in Appendix C. Here, the inductances in the network are increased by a factor of four, which implies that the nonlinear circuits are coupled more weakly as compared to the previous case. For this set of parameters, we obtain $\|\mathcal{F}(z_{\rm ckt}(\mathrm{j}\omega), y_{\rm series}^{-1}(\mathrm{j}\omega)\lambda_j\|_\infty \sigma \not< 1$, $j = 2, 3, 4$, and the sufficient condition (24) is violated. While this is not an indication that the terminal voltages cannot synchronize, it turns out that in this case, the terminal voltages indeed do not synchronize. With the same set of initial conditions as before, we plot the the terminal voltages and the voltage synchronization error in Fig. 9 for this network.

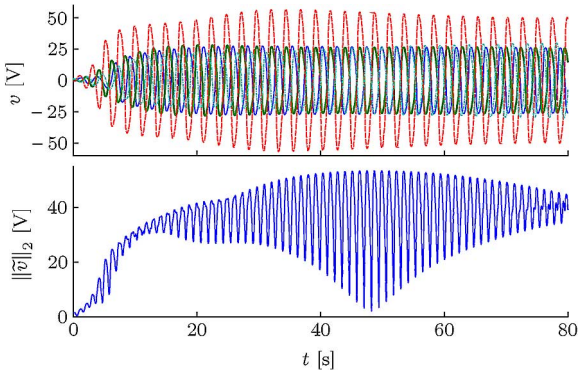

Fig. 9. Terminal voltages $v(t)$ and synchronization error $\|\widetilde{v}(t)\|_2$ when condition (24) fails, $\|\mathcal{F}(z_{\rm ckt}(\mathrm{j}\omega), y_{\rm series}^{-1}(\mathrm{j}\omega)\lambda_j\|_\infty \sigma \not< 1$, $j = 2, 3, 4$, and synchronization is not guaranteed.

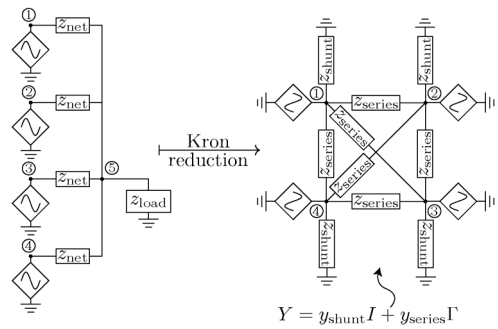

Fig. 10. Network composed of nonlinear electrical circuits connected to a common load through identical branch impedances, and the corresponding Kron-reduced circuit. Homogeneity of the original electrical network implies that the admittance matrix of the Kron-reduced network is given by $Y = y_{\rm shunt} I + y_{\rm series} \Gamma$.

B. Homogeneous Network With Shunt Load

The network topology examined here is illustrated in Fig. 10. The network branch impedance is given by $z_{\rm net}(s) = sL_{\rm net} + R_{\rm net}$. The impedance of the shunt load connected to the internal node is denoted by $z_{\rm load}(s)$. This is an example of a homogeneous network since the effective impedances between any two nonlinear circuits are identical, and the effective impedances between the nonlinear circuits and electrical ground are also identical (see Section VI-A). In particular

$$z_{\rm eff-series} = 2z_{\rm net}, \quad z_{\rm eff-shunt} = z_{\rm net} + z_{\rm load}. \tag{45}$$

Following Lemma 4, we obtain the Kron-reduced network (also illustrated in Fig. 10) with admittance matrix given by $Y = y_{\rm shunt} I + y_{\rm series} \Gamma$. By applying (37), we obtain

$$\begin{aligned} y_{\rm shunt} &= (z_{\rm net} + 4z_{\rm load})^{-1} \\ y_{\rm series} &= z_{\rm load} \left(z_{\rm net}(z_{\rm net} + 4z_{\rm load})^{-1}\right)^{-1}. \end{aligned} \tag{46}$$

Substituting $y_{\rm shunt}$ and $y_{\rm series}$ in (42), we obtain the following sufficient condition for synchronization in this network:

$$\left\|\mathcal{F}\left(z_{\rm ckt}, z_{\rm net}^{-1}\right)\right\|_\infty \sigma = \left\| \frac{z_{\rm ckt}(\mathrm{j}\omega) z_{\rm net}(\mathrm{j}\omega)}{z_{\rm ckt}(\mathrm{j}\omega) + z_{\rm net}(\mathrm{j}\omega)} \right\|_\infty \sigma < 1. \tag{47}$$

It is instructive to explore the impact of the network parameters $R_{\rm net}$ and $L_{\rm net}$ on the synchronization condition (47). Fig. 11 shows $\xi(R_{\rm net}, L_{\rm net}) := \|\mathcal{F}(z_{\rm ckt}, z_{\rm net}^{-1})\|_\infty \sigma$ for a range of parameter values. For sufficiently low values of $R_{\rm net}$ and $L_{\rm net}$, $\xi(R_{\rm net}, L_{\rm net}) < 1$ and synchronization is guaranteed.

Consider now, the asymptotic behavior of $\xi(R_{\rm net}, L_{\rm net})$. Particularly, we will focus on two points [a] and [b] that are marked in Fig. 11. Fig. 12 depicts the magnitude of

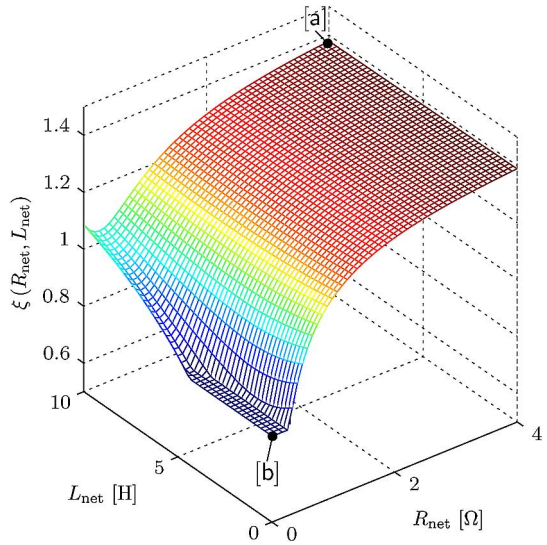

Fig. 11. The function, $\xi(R_{\rm net}, L_{\rm net})$ plotted for a range of values of $R_{\rm net}$ and $L_{\rm net}$. Synchronization is guaranteed for values of $R_{\rm net}$ and $L_{\rm net}$ where $\xi(R_{\rm net}, L_{\rm net}) < 1$.

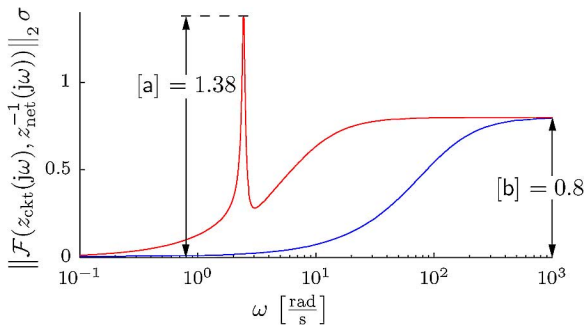

Fig. 12. Magnitude of $\mathcal{F}(z_{\rm ckt}(\mathrm{j}\omega), z_{\rm net}^{-1}(\mathrm{j}\omega))\sigma$ as a function of ω.

$\mathcal{F}(z_{\rm ckt}(\mathrm{j}\omega), z_{\rm net}^{-1}(\mathrm{j}\omega))\sigma$ as a function of frequency, ω, for two representative values of $R_{\rm net}, L_{\rm net}$; corresponding to the asymptotes [a] and [b]. The effect of reducing the values of $R_{\rm net}, L_{\rm net}$ (which increases the coupling between the circuits) also translates to damping the peak of the magnitude response. Synchronization is guaranteed when the peak is less than unity.

C. Impact of Network Size and Topology on Synchronization

In general, it is difficult to study the impact of the network size or topology on the feasibility of our synchronization conditions since closed-form solutions for the $\mathcal{H}_\infty$ norm may not be available. However, for resistive networks a complete analytic treatment is possible.

As a particular example, consider a set of N dead-zone oscillators as in Fig. 2(b) connected through a resistive network. The linear subsystem impedances $z_{\rm ckt}(\mathrm{j}\omega)$ of the oscillators are given in (44) and the parameter values are listed in Appendix D. To ensure periodic oscillations in steady-state, it is necessary to pick (see [4] for details):

$$\sigma > 1/R. \tag{48}$$

The dead-zone oscillators are connected through a resistive electrical network with identical branch conductances

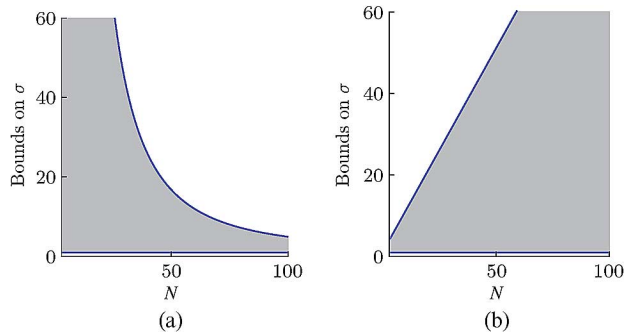

Fig. 13. Upper and lower bounds on σ to guarantee asymptotic synchronization of periodic waveforms as a function of the number of dead-zone oscillators interconnected in a (a) ring and (b) all-to-all graph topology. Shaded region denotes feasible values of σ.

$y_{\rm series}(\mathrm{j}\omega) =: r^{-1}$, no internal nodes, and a topology to be specified later. In the resistive case, the relevant synchronization conditions from Theorem 2 then reduce to

$$\left\|\mathcal{F}\left(z_{\rm ckt}(\mathrm{j}\omega), \lambda_2(N)/r\right)\right\|_\infty \sigma < 1 \tag{49}$$

where $\lambda_2(N)$ is the algebraic connectivity of the underlying network parameterized by the number of nodes N. After substituting $z_{\rm ckt}(\mathrm{j}\omega)$ in the definition of the linear fractional transformation, we obtain

$$\mathcal{F} = \left(\frac{1}{R} + \frac{\lambda_2(N)}{r} + \mathrm{j}\left(\omega C - \frac{1}{\omega L}\right)\right)^{-1}. \tag{50}$$

For the $\mathcal{H}_\infty$-norm, it follows that

$$\left\|\mathcal{F}\left(z_{\rm ckt}(\mathrm{j}\omega), y_{\rm series}(\mathrm{j}\omega)\lambda_2(N)\right)\right\|_\infty = \left(\frac{1}{R} + \frac{\lambda_2(N)}{r}\right)^{-1}. \tag{51}$$

Therefore, the conditions in (49) reduce to:

$$\left(\frac{1}{R} + \frac{\lambda_2(N)}{r}\right)^{-1} \sigma < 1. \tag{52}$$

Condition (48) provides a lower bound on σ to ensure periodic oscillations, and (52) provides an upper bound on σ to ensure synchronization in steady state. Taken together, to ensure periodic oscillations *and* synchronized waveforms, the gain σ must be picked such that

$$\frac{1}{R} < \sigma < \frac{1}{R} + \frac{\lambda_2(N)}{r}. \tag{53}$$

Notice that the range of permitted values for σ patently depends on the network topology as well as the size of the network. As a case study, consider the all-to-all and ring topologies, for which the algebraic connectivities satisfy

$$\lambda_2(N) = \begin{cases} N & \text{all-to-all} \\ 2 - 2\cos\left(\frac{2\pi}{N}\right) & \text{ring.} \end{cases} \tag{54}$$

For the ring topology, it is clear that λ_2 is a decreasing function of N, while for the all-to-all topology, λ_2 is an increasing function of N. Since the upper bound (52) is affine in $\lambda_2(N)$, these scaling laws are directly reflected in the feasibility of the bounds in (53) for the two topologies, see Figs. 13(a) and (b) for an illustration.

VIII. Concluding Remarks and Directions for Future Work

We derived a synchronization condition for a class of nonlinear electrical circuits coupled through passive LTI electrical networks. We considered particular classes of networks, where perfect synchronization of the terminal voltages can be achieved. These classes included homogeneous networks and networks with uniform line characteristics—both with and without shunt elements. Whereas these classes of networks seem to be restrictive at first, it is the belief of the authors that—with the present setup—perfect synchronization cannot be achieved for more general and heterogeneous networks, where the nonlinear circuits are possibly non-identical and support different loads. In this case, the subsystems have no common asymptotic dynamics to synchronize on [36].

In ongoing and future work, we plan to address the problems of synchronization in heterogeneous networks and the regulation of the asymptotic synchronized dynamics. Further topics of interest include the analysis of Kron reduction of general RLC circuits (including pathological cases) and synchronization through directed and possibly nonlinear electrical networks. Note also, that the bounds for synchrony that we obtain will not always be tight since the small gain theorem condition that we employ is sufficient to synchronize a wide range of systems. In future work, we aim to reduce the degree of conservatism even further through the use of integral quadratic constraints. In addition, a compelling direction for further work relates to investigating the impact of the number of nodes, type of interconnecting impedances, type of nonlinear circuits, and graph topology on the ease with which synchronization protocols can be formulated (the case study in Section VII-C provided a motivating example in this regard).

Appendix

A. Kron Reduction of Complex-Symmetric Matrices

In this appendix, we discuss the Kron reduction of complex-valued admittance matrices and the properties of the effective impedances. The following results are extensions from the real-valued and symmetric cases considered in [13], to complex-symmetric (and not necessarily Hermitian) settings relevant in this work. Since only a subset of results in [13] directly carries over to the complex-symmetric case, we present self-contained statements with brief proof sketches. These results directly lead up to Lemmas 2 and 4 in this paper.

First, notice that an admittance matrix $Y_{\mathcal{A}}$ without shunt elements is singular due to zero row and column sums, and an admittance matrix with at least one shunt element is invertible due to irreducibly block diagonally dominance [31, Corollary 6.2.27]. To analyze regular and singular admittance matrices simultaneously, we associate an *augmented admittance matrix* $\widehat{Y}_{\mathcal{A}}$ to a regular admittance matrix $Y_{\mathcal{A}}$:

$$\widehat{Y}_{\mathcal{A}} := \left[\begin{array}{ccc|c} & & & -y_1 \\ & Y_{\mathcal{A}} & & \vdots \\ & & & -y_{|\mathcal{A}|} \\ \hline -y_1 & \cdots & -y_{|\mathcal{A}|} & \sum_{m=1}^{|\mathcal{A}|} y_m \end{array}\right] \tag{55}$$

The augmented admittance matrix $\widehat{Y}_{\mathcal{A}}$ corresponds to the case when the ground is modeled as an additional node with index $|\mathcal{A}|+1$ and zero voltage. Notice that $\widehat{Y}_{\mathcal{A}}$ is singular with zero row and column sums. Likewise, a singular admittance matrix resulting from a network without shunt elements can be regularized by grounding an arbitrary node. We denote the Kron-reduced matrix associated to $\widehat{Y}_{\mathcal{A}}$ by $\widehat{Y}$. As it turns out, the augmentation process and the Kron reduction commute.

Lemma 5: Consider a singular admittance matrix $Y_{\mathcal{A}}$, its augmented matrix $\widehat{Y}_{\mathcal{A}}$, and their associated Kron-reduced matrices Y and $\widehat{Y}$, respectively. The following diagram commutes:

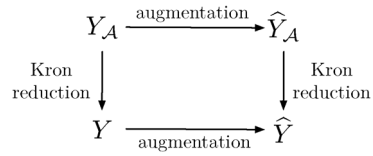

Proof: The proof is analogous to the proof of [13, Lemma III.1, Property 3]. The result in [13] relies on the Quotient Formula [32, Theorem 1.4] which extends to complex-valued matrices, as well as the closure of symmetry and zero row (column) sums under Kron reduction (shown in Theorem 1). ■

As the next key property, we establish that the effective impedances z_{nm} among the boundary nodes $n, m \in \mathcal{N}$ are invariant under Kron reduction and augmentation.

Theorem 3: Consider the admittance matrix $Y_{\mathcal{A}}$ and the Kron-reduced matrix Y. The following statements hold:

1) Invariance under Kron reduction: the effective impedance between any two boundary nodes is equal when computed from Y or $Y_{\mathcal{A}}$, that is, for any $n, m \in \{1, \ldots, N\}$

$$\begin{aligned} z_{nm} &= (e_n - e_m)^{\mathrm{T}} Y^{\dagger} (e_n - e_m) \\ &\equiv (e_n - e_m)^{\mathrm{T}} Y_{\mathcal{A}}^{\dagger} (e_n - e_m). \end{aligned} \tag{56}$$

2) Invariance under augmentation: if $Y_{\mathcal{A}}$ is a nonsingular matrix, then the effective impedance is equal when computed from $Y_{\mathcal{A}}$ or $\widehat{Y}_{\mathcal{A}}$, that is, for any $n, m \in \{1, \ldots, |\mathcal{A}|\}$

$$\begin{aligned} z_{nm} &= (e_n - e_m)^{\mathrm{T}} Y_{\mathcal{A}}^{-1} (e_n - e_m) \\ &\equiv (e_n - e_m)^{\mathrm{T}} \widehat{Y}_{\mathcal{A}}^{\dagger} (e_n - e_m). \end{aligned} \tag{57}$$

Equivalently, statements 1) and 2) imply that, if $Y_{\mathcal{A}}$ is a regular admittance matrix, then the following diagram commutes:

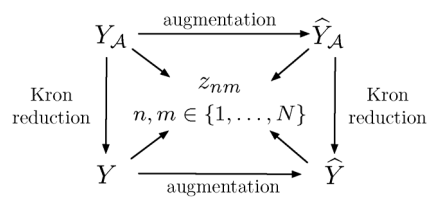

Proof: To prove Theorem 3, we first establish some matrix identities. We need the following identity for a singular admittance matrix $Y \in \mathbb{C}^{N \times N}$ and a real nonzero number δ:

$$\left(Y + \left(\frac{\delta}{N}\right) \mathbf{1}\mathbf{1}^{\mathrm{T}}\right)^{-1} = Y^{\dagger} + \left(\frac{1}{\delta N}\right) \mathbf{1}\mathbf{1}^{\mathrm{T}}. \tag{58}$$

Using the projector formula (for a singular admittance matrix) $YY^{\dagger} = Y^{\dagger}Y = \Pi$, the identity (58) can be verified since the

product of the left-hand and the right-hand side of (58) equal the identity matrix. If a singular admittance matrix $Y \in \mathbb{C}^{N\times N}$ is of dimension $N \geq 3$, then by taking the Nth node as a reference and deleting the associated Nth column and Nth row, we obtain the nonsingular matrix $\overline{Y} \in \mathbb{C}^{(N-1)\times(N-1)}$. As suggested by physical intuition, the effective impedance among the nodes $n, m \in \{1, \ldots, N-1\}$ is not affected by grounding the Nth node, that is, for all $n, m \in \{1, \ldots, N-1\}$

$$\begin{aligned} z_{nm} &= (e_n - e_m)^{\mathrm{T}} \overline{Y}^{-1} (e_n - e_m) \\ &\equiv (e_n - e_m)^{\mathrm{T}} Y^{\dagger} (e_n - e_m). \end{aligned} \tag{59}$$

The identity (59) can be verified by using the formula $\overline{Y}^{-1}_{nm} = Y^{\dagger}_{nm} - Y^{\dagger}_{nN} - Y^{\dagger}_{mN} + Y^{\dagger}_{NN}$ [37, Appendix B, formula (17)] whose derivation extends to the complex-valued case.

To prove statement 1), consider first the case when $Y_{\mathcal{A}}$ is invertible due to presence of shunt admittances. Recall that we are interested in the effective impedances only among the boundary nodes, that is, the leading principal $(N \times N)$-block of $Y^{\dagger}_{\mathcal{A}} = Y^{-1}_{\mathcal{A}}$. The Schur complement formula [32, Theorem 1.2] gives the leading $(N \times N)$-block of $Y^{-1}_{\mathcal{A}}$ as the inverse Schur complement Y^{-1}. It follows that, for all $n, m \in \{1, \ldots, N\}$,

$$\begin{aligned} z_{nm} &= (e_n - e_m)^{\mathrm{T}} Y^{-1} (e_n - e_m) \\ &\equiv (e_n - e_m)^{\mathrm{T}} Y^{-1}_{\mathcal{A}} (e_n - e_m). \end{aligned} \tag{60}$$

On the other hand, if $Y_{\mathcal{A}}$ is singular due to absence of shunt admittances, an analogous reasoning applies on the image of Y and using the identity (58), or after grounding an arbitrary interior node (i.e., regularizing $Y_{\mathcal{A}}$) and using the identity (59), see the proof of [13, Theorem III.8, Property 1] for details.

To prove statement 2), notice that the regular admittance matrix $Y_{\mathcal{A}}$ with shunt elements is the leading principal $(|\mathcal{A}| \times |\mathcal{A}|)$-block of the augmented singular admittance matrix $\widehat{Y}_{\mathcal{A}}$. Statement 2) follows then directly from identity (59) after replacing N, Y, and $\overline{Y}$ with $N+1$, $\widehat{Y}_{\mathcal{A}}$, and $Y_{\mathcal{A}}$. ■

Theorem 4: Consider an admittance matrix $Y_{\mathcal{A}}$ and its Kron-reduced matrix Y. Consider the following two cases:

1) *No shunt elements*: Assume that $Y_{\mathcal{A}}$ is singular due to the absence of shunt elements. Let $Z \in \mathbb{C}^{N\times N}$ be the matrix of effective impedances. The following statements are equivalent:
   - (i) The effective impedances among the boundary nodes $\{1, \ldots, N\}$ are uniform, that is, there is $z_{\mathrm{eff}} \in \mathbb{C} \setminus \{0\}$ such that $z_{nm} = z_{\mathrm{eff}}$ for all distinct $n, m \in \{1, \ldots, N\}$;
   - (ii) The branch admittances in the Kron-reduced network take the uniform value $y_{\mathrm{series}} \in \mathbb{C} \setminus \{0\}$, that is, $Y = y_{\mathrm{series}} \Gamma$.

   If statements (i) and (ii) are true, then $z_{\mathrm{eff}} = 2/N y_{\mathrm{series}}$.
2) *Shunt elements*: Assume that $Y_{\mathcal{A}}$ is regular due to the presence of shunt elements. Consider the grounded node $|\mathcal{A}|+1$ and the augmented admittance matrices $\widehat{Y}_{\mathcal{A}}$ and $\widehat{Y}$. Let $Z \in \mathbb{R}^{(|\mathcal{A}|+1)\times(|\mathcal{A}|+1)}$ be the matrix of effective impedances in the augmented network. The following statements are equivalent:
   - (iii) The effective impedances both among the boundary nodes $\{1, \ldots, N\}$ and between all boundary nodes $\{1, \ldots, N\}$ and the grounded node $|\mathcal{A}| + 1$ are uniform, that is, there are $z_{\mathrm{eff-series}} \in \mathbb{C} \setminus \{0\}$ and $z_{\mathrm{eff-shunt}} \in \mathbb{C} \setminus \{0\}$ satisfying $z_{\mathrm{eff-series}}/z_{\mathrm{eff-shunt}} \neq 2N/N - 1$ such that $z_{ij} = z_{\mathrm{eff-series}}$ for all distinct $n, m \in \{1, \ldots, N\}$ and $z_{n,|\mathcal{A}|+1} = z_{\mathrm{eff-shunt}}$ for all $n \in \{1, \ldots, N\}$.
   - (iv) The branch and shunt admittances in the Kron-reduced network are uniform, that is, there are $y_{\mathrm{series}} \in \mathbb{C} \setminus \{0\}$ and $y_{\mathrm{shunt}} \in \mathbb{C} \setminus \{0\}$ satisfying $y_{\mathrm{shunt}} \neq -N y_{\mathrm{series}}$ such that $Y = y_{\mathrm{shunt}} I + y_{\mathrm{series}} \Gamma$.

   If statements (iii) and (iv) are true, then

$$z_{\mathrm{eff-series}} = \frac{2}{N y_{\mathrm{series}} + y_{\mathrm{shunt}}} \tag{61}$$

$$z_{\mathrm{eff-shunt}} = \frac{y_{\mathrm{shunt}} + y_{\mathrm{series}}}{y_{\mathrm{shunt}}(N y_{\mathrm{series}} + y_{\mathrm{shunt}})}. \tag{62}$$

The admittance assumption $y_{\mathrm{shunt}} \neq -N y_{\mathrm{series}}$ (and the equivalent assumption $z_{\mathrm{eff-series}}/z_{\mathrm{eff-shunt}} \neq 2N/N - 1$ for the effective impedances) guarantees regularity (respectively a single zero eigenvalue) of the admittance matrix. As discussed in Section VI-A, this assumption is practically not restrictive.

Proof of Theorem 4: Here, we present the proof strategy for case 1). Due to the invariance of the effective impedance (and Kron reduction) under the augmentation process (see Lemma 5 and Theorem 3), an analogous reasoning and similar formulae apply to case 2), see [13].

We first prove the statement $(i) \implies (ii)$: Notice that $Z = Z^{\mathrm{T}}$ has zero diagonal elements and $Y^{\dagger}$ is symmetric with zero row and column sums. Hence, both matrices have $N(N-1)/2$ independent elements, and the linear formula relating the elements z_{nm} and $Y^{\dagger}_{nm}$ can be inverted [13, identity (34)]:

$$Y^{\dagger}_{nm} = -\frac{1}{2}\left(z_{nm} - \frac{1}{N}\sum_{k=1}^{N}(z_{nk} + z_{mk}) + \frac{1}{N^2}\sum_{k,\ell=1}^{N} z_{k\ell} \right). \tag{63}$$

From the above formula, it can be readily verified that a uniform effective impedance matrix, $Z = z_{\mathrm{eff}}(\mathbf{1}\mathbf{1}^{\mathrm{T}} - I)$, yields a uniform inverse matrix $Y^{\dagger} = z_{\mathrm{eff}}/(2N)\Gamma$. It is worth mentioning that for an admittance matrix with uniform branch admittances, $Y = y_{\mathrm{series}}\Gamma$, the pseudo inverse $Y^{\dagger}$ is again an admittance matrix with uniform branch admittances given by

$$Y^{\dagger} = (y_{\mathrm{series}}\Gamma)^{\dagger} = \frac{1}{(N^2 y_{\mathrm{series}})\Gamma}. \tag{64}$$

Identity (64) can be verified since Y and $Y^{\dagger}$ satisfy the Penrose equations. According to (64), this uniform inverse matrix $Y^{\dagger} = z_{\mathrm{eff}}/(2N)\Gamma$ yields the uniform admittance matrix $Y = 2/(N z_{\mathrm{eff}})\Gamma$.

Now we consider the converse implication $(ii) \implies (i)$. Due to Theorem 3 the effective impedance is invariant under Kron reduction. In this case, substituting $Y^{\dagger}$ from (64) in (8), we see that the effective impedances are given by

$$\begin{aligned} z_{nm} &= \frac{1}{(N^2 y_{\mathrm{series}})}(e_n - e_m)^{\mathrm{T}}(NI - \mathbf{1}\mathbf{1}^{\mathrm{T}})(e_n - e_m) \\ &= \frac{2}{N y_{\mathrm{series}}} = z_{\mathrm{eff}}, \forall n, m \in \{1, \ldots, N\}. \end{aligned} \tag{65}$$

Hence, the $N(N-1)/2$ pairwise effective impedances z_{nm} between the boundary nodes are uniform. ■

B. Parameters of Chua's Circuits

Linear subsystem parameters [30]: $R = 10/7\ \Omega$, $L = 1/7$ H, $C_{\rm a} = 1/9$ F, $C_{\rm b} = 1$ F.

Nonlinear-subsystem parameters: $\sigma_0 = -0.8$ S, $\sigma_1 = -0.5$ S, $\sigma_2 = 0.8$ S, $\varphi_0 = 1$ V, $\varphi_1 = 14$ V.

C. Lossless Network Parameters

Guaranteed Synchronization: $L_{12} = 0.834$ H, $L_{15} = 0.671$ H, $L_{26} = 0.277$ H, $L_{56} = 1.0575$ H, $L_{45} = 0.3655$ H, $L_{46} = 1.0245$ H, $L_{36} = 0.3240$ H, $L_{67} = 0.4735$ H, $L_{37} = 0.1875$ H, $L_{47} = 0.74$ H.

No Guarantee on Synchronization: $L_{12} = 3.336$ H, $L_{15} = 2.684$ H, $L_{26} = 1.108$ H, $L_{56} = 4.23$ H, $L_{45} = 1.462$ H, $L_{46} = 4.098$ H, $L_{36} = 1.296$ H, $L_{67} = 1.894$ H, $L_{37} = 0.75$ H, $L_{47} = 2.96$ H.

D. Parameters of Dead-Zone Oscillators

Linear subsystem parameters: $R = 1\ \Omega$, $L = 1$ H, $C = 1$ F. Network-branch impedance: $r = 10^{-3}\ \Omega$ (ring topology), $r = 1\ \Omega$ (all-to-all topology).

REFERENCES

[1] S. H. Strogatz, "Nonlinear dynamics and chaos: With applications to physics, biology, chemistry, engineering," in *Studies in Nonlinearity*, 1st ed. : Westview Press, Jan. 2001.

[2] F. Dörfler and F. Bullo, "Synchronization in complex oscillator networks: A survey," *Automatica*, vol. 50, no. 6, pp. 1539–1564, 2014.

[3] L. A. B. Tôrres, J. P. Hespanha, and J. Moehlis, "Power supplies synchronization without communication," in *Proc. Power and Energy Society General Meeting*, Jul. 2012.

[4] B. B. Johnson, S. V. Dhople, A. O. Hamadeh, and P. T. Krein, "Synchronization of nonlinear oscillators in an LTI power network," *IEEE Trans. Circuits Syst. I, Reg. Papers*, vol. 61, pp. 834–844, Mar. 2014.

[5] B. B. Johnson, S. V. Dhople, J. Cale, A. O. Hamadeh, and P. T. Krein, "Oscillator-based inverter control for islanded three-phase microgrids," *IEEE J. Photovolt.*, vol. 4, pp. 387–395, Jan. 2014.

[6] B. B. Johnson, S. V. Dhople, A. O. Hamadeh, and P. T. Krein, "Synchronization of parallel single-phase inverters using virtual oscillator control," *IEEE Trans. Power Electron.*, vol. 29, no. 11, pp. 6124–6138, Nov. 2014.

[7] L. O. Chua and G. N. Lin, "Canonical realization of Chua's circuit family," *IEEE Trans. Circuits Syst.*, vol. 37, pp. 885–902, Jul. 1990.

[8] J. Gismero and J. Perez, "Harmonic describing function: Application to microwave oscillator's design," in *Proc. Eur. Microw. Conf.*, 1990, vol. 2, pp. 1213–1218.

[9] L. Chua, "Passivity and complexity," *IEEE Trans. Circuits Syst. I: Fundam. Theory Appl.*, vol. 46, pp. 71–82, Jan. 1999.

[10] I. M. Kyprianidis, P. Haralabidis, and I. N. Stouboulos, "Controlling and synchronization of a second-order non-autonomous nonlinear electric circuit," in *Proc. IEEE Int. Conf. Electronics, Circuits Syst.*, 1999, vol. 3, pp. 1247–1251.

[11] R. P. Malhame, "Negative resistance oscillators revisited," in *Proc. IEEE Int. Conf. Electronics, Circuits Syst.*, 2000, vol. 1, pp. 202–205.

[12] I. M. Kyprianidis and I. N. Stouboulos, "Chaotic and hyperchaotic synchronization of two nonautonomous and nonlinear electric circuits," in *Proc. IEEE Int. Conf. Electronics, Circuits Syst.*, 2001, vol. 3, pp. 1351–1354.

[13] F. Dörfler and F. Bullo, "Kron reduction of graphs with applications to electrical networks," *IEEE Trans. Circuits Syst. I, Reg. Papers*, vol. 60, pp. 150–163, Jan. 2013.

[14] A. Hamadeh, G.-B. Stan, and J. Gonçalves, "Constructive Synchronization of Networked Feedback Systems," in *Proc. IEEE Conf. Decision Contr.*, Dec. 2010, pp. 6710–6715.

[15] A. Hamadeh, "Constructive Robust Synchronization of Networked Control Systems," Ph.D. dissertation, Cambridge Univ., Cambridge, UK, Jun. 2010.

[16] A. Dhawan, A. Hamadeh, and B. Ingalls, "Designing synchronization protocols in networks of coupled nodes under uncertainty," in *Proc. Amer. Contr. Conf.*, Jun. 2012, pp. 4945–4950.

[17] C. W. Wu and L. O. Chua, "Synchronization in an array of linearly coupled dynamical systems," *IEEE Trans. Circuits Syst. I, Fundam. Theory Appl.*, vol. 42, pp. 430–447, Aug. 1995.

[18] C. W. Wu, "Synchronization in arrays of chaotic circuits coupled via hypergraphs: Static and dynamic coupling," in *Proc. IEEE ISCAS*, 1998, vol. 3, pp. 287–290.

[19] A. Pogromsky and H. Nijmeijer, "Cooperative oscillatory behavior of mutually coupled dynamical systems," *IEEE Trans. Circuits Syst. I, Fundam. Theory Appl.*, vol. 48, pp. 152–162, Feb. 2001.

[20] G.-B. Stan, "Global Analysis and Synthesis of Oscillations: A Dissipativity Approach," Ph.D. dissertation, Univ. Liege, Liege, Belgium, May 2005.

[21] C. W. Wu, "Synchronization in arrays of coupled nonlinear systems with delay and nonreciprocal time-varying coupling," *IEEE Trans. Circuits Syst. II, Exp. Briefs*, vol. 52, pp. 282–286, May 2005.

[22] M. Arcak, "Passivity as a design tool for group coordination," *IEEE Trans. Autom. Contr.*, vol. 52, pp. 1380–1390, Aug. 2007.

[23] G.-B. Stan and R. Sepulchre, "Analysis of interconnected oscillators by dissipativity theory," *IEEE Trans. Autom. Contr.*, vol. 52, pp. 256–270, Feb. 2007.

[24] W. Yu, J. Cao, and J. Lü, "Global synchronization of linearly hybrid coupled networks with time-varying delay," *SIAM J. Appl. Dynamical Syst.*, vol. 7, no. 1, pp. 108–133, 2008.

[25] A. Hamadeh, G.-B. Stan, R. Sepulchre, and J. Goncalves, "Global state synchronization in networks of cyclic feedback systems," *IEEE Trans. Autom. Contr.*, vol. 57, pp. 478–483, Feb. 2012.

[26] G. Kron, *Tensor Analysis on Networks*. New York, NY, USA: Wiley, 1939.

[27] A. Van der Schaft, "L2-gain and passivity techniques in nonlinear control," in *Lecture Notes in Control and Information Sciences*. London, U.K.: Springer, 1996.

[28] H. Khalil, *Nonlinear Systems*, 3rd ed. Upper Saddle River, NJ, USA: Prentice Hall, 2002.

[29] K. Zhou, J. Doyle, and K. Glover, *Robust and Optimal Control*. Upper Saddle River, NJ, USA: Prentice Hall, 1996.

[30] T. Matsumoto, L. O. Chua, and M. Komuro, "The double scroll," *IEEE Trans. Circuits Systems*, vol. 32, pp. 797–818, Aug. 1985.

[31] R. A. Horn and C. R. Johnson, *Matrix Analysis*. Cambridge, U.K.: Cambridge Univ. Press, 2012.

[32] F. Zhang, *The Schur Complement and Its Applications*. New York, NY, USA: Springer, 2005, vol. 4.

[33] E. I. Verriest and J. C. Willems, "The behavior of linear time invariant RLC circuits," in *Proc. IEEE Conf. Decision Contr.*, 2010, pp. 7754–7758.

[34] S. Y. Caliskan and P. Tabuada, "Kron Reduction of Generalized Electrical Networks," 2012 [Online]. Available: http://arxiv.org/abs/1207.0563

[35] M. Fiedler, "Algebraic connectivity of graphs," *Czechoslovak Math. J.*, vol. 23, no. 2, pp. 298–305, 1973.

[36] P. Wieland, J. Wu, and F. Allgöwer, "On synchronous steady states and internal models of diffusively coupled systems," *IEEE Trans. Automatic Contr.*, May 2013, to be published.

[37] F. Fouss, A. Pirotte, J.-M. Renders, and M. Saerens, "Random-walk computation of similarities between nodes of a graph with application to collaborative recommendation," *IEEE Trans. Knowledge Data Eng.*, vol. 19, no. 3, pp. 355–369, 2007.

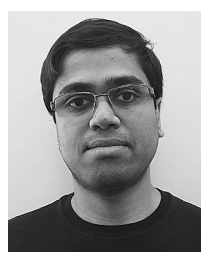

Sairaj V. Dhople (S'09–M'13) received the B.S., M.S., and Ph.D. degrees in electrical engineering, in 2007, 2009, and 2012, respectively, from the University of Illinois, Urbana-Champaign, IL, USA.

He is currently an Assistant Professor in the Department of Electrical and Computer Engineering at the University of Minnesota Minneapolis, MN, USA, where he is affiliated with the Power and Energy Systems research group. His research interests include modeling, analysis, and control of power electronics and power systems with a focus on renewable integration.

Brian B. Johnson (S'08–M'13) received the B.S. degree in physics from Texas State University, San Marcos, TX, USA, in 2008. He received the M.S. and Ph.D. degrees in electrical and computer engineering from the University of Illinois at Urbana-Champaign, IL, USA, in 2010 and 2013, respectively.

He is currently an Electrical Engineer with the National Renewable Energy Laboratory in Golden, CO, USA. He was awarded a National Science Foundation Graduate Research Fellowship in 2010. His research interests are in power electronics, distributed generation, renewable energy systems, and controls.

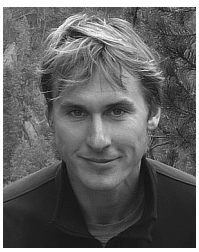

Florian Dörfler (S'09–M'13) received the Ph.D. degree in mechanical engineering from the University of California at Santa Barbara, CA, USA, in 2013, and a Diploma degree in engineering cybernetics from the University of Stuttgart, Stuttgart, Germany, in 2008.

He is an Assistant Professor at the Automatic Control Laboratory at ETH Zürich. From 2013 to 2014 he was an Assistant Professor at the University of California Los Angeles, Los Angeles, CA, USA. His primary research interests are centered around distributed control, complex networks, and cyber-physical systems with applications to smart power grids and robotic coordination.

Dr. Dörfler is a recipient of the the 2010 ACC Student Best Paper Award, the 2011 O. Hugo Schuck Best Paper Award, and the 2014 Automatica Best Paper Award. As a co-advisor and a co-author, he has been a finalist for the ECC 2013 Best Student Paper Award.

Abdullah O. Hamadeh received the M.Eng., M.A. and Ph.D. degrees in electrical engineering from the University of Cambridge, Cambridge, MA, USA, in 2005, 2008, and 2010 respectively. His doctoral research was in the control and synchronization of networked dynamical systems.

Between 2010 and 2013 he held post-doctoral positions at the University of Waterloo and at Rutgers University, and he is currently a Post-Doctoral Associate at the Department of Mechanical Engineering at the Massachusetts Institute of Technology. His current research interests are in the applications of control theoretic techniques to systems and synthetic biology and in the control of electrical power networks.